

Equilibrium Molecular Dynamics Calculations of the Transport Properties of Molten Uranium Dioxide and Zirconium¹

M. Katahira^{2,3} and Y. Nagasaka²

Viscosity and thermal conductivity of uranium dioxide and zirconium in molten state have been calculated by means of equilibrium molecular dynamics simulation (EMD). The potential function of uranium dioxide employed is partially ionic model, which consists of the Coulomb interaction, core repulsion and Morse type potential. That of zirconium is *N*-body potential, which consists of the Born-Mayer pairwise interaction and the attractive interaction derived within a second moment approximation of the tight binding energy. Transport properties of UO₂ and Zr were calculated by using the generalized Einstein equation based on Green-Kubo equation. In the present study we have calculated viscosity and thermal conductivity of molten UO₂ at high temperatures up to 3400 K. Calculated thermal conductivity of molten UO₂ show eight times as large as experimental values at most. Calculated viscosity of molten UO₂ are in good agreement with Tasman's experimental data within 30%. Viscosity of molten Zr are calculated up to 2600 K, where no experimental data exists.

KEY WORDS: molecular dynamics, molten uranium dioxide, molten zirconium thermal conductivity, viscosity

1. INTRODUCTION

Transport properties of molten uranium dioxide (UO₂) and molten zirconium (Zr) are needed in order to analyze corium movement in various potential accident situations for designing advanced safer nuclear reactor. Corium is the melted core of nuclear reactor, which consists of UO₂, ZrO₂, Zr, Fe, and fission products. UO₂ is used as the nuclear fuel and Zr is used as zircaloy for covering the fuel. The constituent materials of corium are mostly UO₂ and Zr. Unfortunately, experimental investigation of the relevant properties is difficult because of their radioactive and the high temperatures involved (melting point of UO₂: 3120K, Zr: 2125K). There have been very limited number of experimental studies on their properties whose discrepancies are far beyond their claimed accuracy. Experimental studies of the viscosity and thermal conductivity of

¹ Paper presented at the Fifteenth Symposium on Thermophysical Properties, June 22-27, 2003, Boulder, Colorado, U.S.A.

² Department of System Design Engineering, Keio University, 3-14-1, Hiyoshi, Yokohama, 223-8522, JAPAN

³ To whom correspondence should be addressed. E-mail: katahira@naga.sd.keio.ac.jp

Table I Experimental studies of transport properties of molten UO₂ and Zr.

Substance	Property	Author	Measurement technique	Temperature range
UO ₂	η	Tsai <i>et al.</i> (1972) [1]	Oscillating Cup Viscometer	3080 K–3260 K
		Woodley (1974) [2]	Oscillating Cup Viscometer	3020 K–3250 K
	λ	Kim <i>et al.</i> (1977) [3]	Modulated Electron Beam	3187 K–3315 K
		Tasman <i>et al.</i> (1983) [4]	Quasistationary method on a partially molten self-contained sample	3120 K–3200 K
Zr	η	Yelviutin <i>et al.</i> (1965) [5]	Oscillating Cup Viscometer	2150 K–2400 K
		Bunnell <i>et al.</i> (1986) [6]	Oscillating Cup Viscometer	2075 K–2175 K
		Paradis <i>et al.</i> (1999) [7]	Electrostatic Levitator	1860 K–2170 K

UO₂ and Zr are listed in Table I.

Several molecular dynamics studies for solid-state properties and structure of UO₂ and Zr have been reported. Super ionic conduction of oxygen ions and properties such as thermal conductivity, compressibility and density had been studied in solid state of UO₂ [8–12]. Temperature dependence of hcp-bcc transition (hcp: hexagonal close packed structure (α), bcc: body-centered cubic structure (β)) and defects, surface and displacement-threshold properties of α -zirconium had been studied in solid state of Zr. [13, 14] However, there is no molecular dynamics study for transport properties of UO₂ and Zr in molten state.

Our final goal is to calculate transport properties of UO₂ and Zr in molten state by using equilibrium molecular dynamics (EMD) simulation.

2. CALCULATION METHODOLOGY OF TRANSPORT PROPERTIES

The calculation methodology of transport properties can be classified into equilibrium molecular dynamics (EMD) and nonequilibrium molecular dynamics (NEMD). In the conventional EMD, the transport properties can be evaluated from the integral of the statistically averaged time correlation function of the momentum flow tensor, the energy current, and particle current in equilibrium state without external disturbance. On the other hand, NEMD uses the current caused by an applied external field. Recently NEMD has been considered as a very efficient tool for calculating transport properties in the case of the complex model. Although NEMD has advantages, the fictitious ex-

ternal field applied to the system seems to be so large that the calculated results may not be used for engineering purposes. Therefore, in the present study we have adopted the EMD method for UO_2 and Zr.

The fluctuation-dissipation theorem relates the decay of macroscopic disturbances, caused by external perturbations, to the spontaneous microscopic fluctuations in a thermodynamical system. This theorem is the basis of the Green-Kubo theory of transport, which equates transport coefficients to correlation functions of microscopically defined fluxes. The expression for viscosity η and thermal conductivity λ can be calculated by using the stress flow tensor τ and energy current J :

$$\eta = \frac{1}{Vk_B T} \int_0^\infty \langle \tau_{xy}(t) \tau_{xy}(0) \rangle dt, \quad (1)$$

$$\lambda = \frac{1}{Vk_B T^2} \int_0^\infty \langle J_x(t) J_x(0) \rangle dt, \quad (2)$$

where τ_{xy} and J_x are

$$\tau_{xy} = \sum_i^N \left[m_i v_{ix} v_{iy} + \frac{1}{2} \sum_{j \neq i}^N F_{xij} y_{ij} \right], \quad (3)$$

$$J_x = \sum_i^N v_{ix} \left[\frac{1}{2} m_i v_i^2 + \frac{1}{2} \phi_{ij}(r_{ij}) \right] + \frac{1}{2} \sum_i^N \sum_{j \neq i}^N \mathbf{v}_i \cdot \mathbf{r}_{ij} F_{ijx}. \quad (4)$$

$\langle \rangle$ denotes equilibrium average, V the volume of system, k_B the Boltzmann constant, T temperature, t time, x_i and y_i the x and y components of the position of particle i , ϕ_{ij} the potential energy between particles i and j , \mathbf{v}_i the velocity vector of particle i , \mathbf{r}_{ij} the position vector between particle i and j , and F_{ijx} the force of x components between particle i and j . The transport properties can be calculated thorough integration of the auto correlation function by GK equation, but calculated values do not show convergence to a certain constant that is theoretically correct when time approaches infinity. Here, we use the following equations [15]:

$$\eta = \lim_{t \rightarrow \infty} \frac{1}{2t} \frac{1}{Vk_B T} \left\langle \left[\int_0^t \tau_{xy}(s) dt \right]^2 \right\rangle, \quad (5)$$

$$\lambda = \lim_{t \rightarrow \infty} \frac{1}{2t} \frac{1}{Vk_B T^2} \left\langle \left[\int_0^t J_x(s) dt \right]^2 \right\rangle. \quad (6)$$

In the above equations, the mean square displacement (MSD) is calculated by means of an integral. Transport properties can be calculated from the slope of MSD. As seen in Fig. 1, transport properties can be calculated from the slope of MSD against time with fewer statistical uncertainties. A clear linear slope was obtained by means of the generalized Einstein equation with less ambiguity.

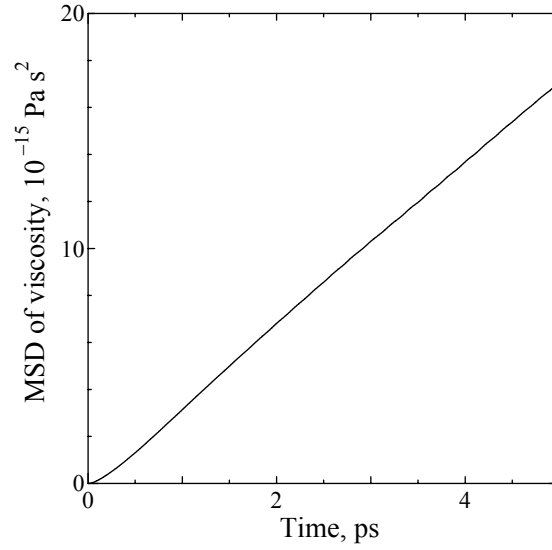


Fig. 1. MSD for viscosity from the GE equation corresponding to Zr at $5904 \text{ kg}\cdot\text{m}^{-3}$ and 2200K .

3. CALCULATION RESULTS OF URANIUM DIOXIDE

The potential function of UO_2 used in the present study is a partially ionic model given by Yamada *et al.* [12], which was the Busing-Ida [16] type potential including a covalent contribution between the nearest anion-cation pair as follows:

$$\phi_{ij} = \frac{Z_i Z_j e^2}{4\pi\epsilon_0 r_{ij}} + f_0 (b_i + b_j) \exp\left(\frac{a_i + a_j - r_{ij}}{b_i + b_j}\right) - \frac{c_i c_j}{r_{ij}^6} + D_{ij} \left\{ \exp[-2\beta_{ij}(r_{ij} - r_{0ij})] - 2 \exp[-\beta_{ij}(r_{ij} - r_{0ij})] \right\} \quad (7)$$

This model consists of the Coulomb interaction, core repulsion, and van der Waals' force. Z_i is the effective partial electronic charges on the ion i , e the electric charge, ϵ_0 the dielectric constant of vacuum. Potential parameters are listed in Table II. The parameters of this model were fitted to thermal diffusivity and compressibility at 1600 K [12]. NVE ensemble calculations were performed for 324 ions (108 cations and 216 anions). The volume of system was chosen so as to reproduce the experimental density at each temperature [17]. The equations of motions were integrated using the velocity Verlet algorithm with a time step Δt of 2 fs. The kinetic energy was kept at desired temperature with scaling the velocities of all ions for the initial 10 ps. Without scaling them the coordinates and velocities obtained for the subsequent 100 ps. Long-range Coulomb interactions were treated with Ewald's summation. Figure 2 shows the mean square displacements of cations and anions obtained from simulations at 3200 K . Several papers reported superionic conduction that anions are diffused at the high temperature in solid state. It is immediately clear from our results for solid that superionic conduction was shown in 3200 K from slope of anions. This solid behavior in liquid temperature and density may be shown because partially ionic model is

too “rigid” for liquid state. The parameters of this model were fitted to the properties of solid state. Furthermore, the parameters were determined to hold the stable CaF_2 type structure and to set the mean square displacement of oxygen ion in the unit cell within 200 pm^2 at 300 K, which was equal to thermal vibration. The parameters were only set to simulating adequately for solid states. In order to simulate liquid state adequately, the interionic model was needed whose parameters were set to not only solid state properties but also those of liquid state such as melting temperature, latent heat, and self diffusion coefficient.

Self diffusion coefficient of anion and cations was calculated from the slope of obtained mean square displacement,

$$D = \lim_{t \rightarrow \infty} \frac{1}{6t} \langle |\mathbf{r}(t) - \mathbf{r}(0)|^2 \rangle. \quad (8)$$

From Fig. 2, the obtained self diffusion coefficient in 3200 K was $6.5 \times 10^{-9} \text{ m}^2/\text{s}$ (ani-

Table II. Parameters of partially ionic model of UO_2 modeled by Yamada *et al.* [12]

Ion	Z_i	a_i	b_i	c_i
		(Å)	(Å)	($\text{kcal}^{1/2} \cdot \text{Å}^3 \cdot \text{mol}^{-1/2}$)
U	-1.2	1.926	0.160	20
O	2.4	1.659	0.160	0

	D_{ij}	β_{ij}	r_0
	($\text{kcal} \cdot \text{mol}^{-1}$)		(Å)
U-O Pairs	18.0	1.25	2.369

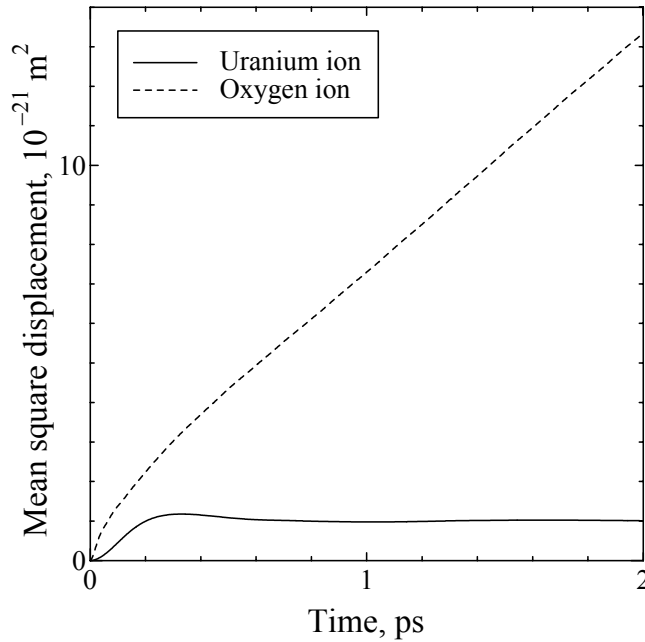


Fig. 2. Mean square displacement of U ions and O ions in 3200 K. Solid line; cations, dash line; anions.

ons). Other studies, calculated value were 1.52×10^{-9} m²/s (anions at 3000 K) by Karakasdis *et al.* [18], 21.1×10^{-9} m²/s (cations) and 35.5×10^{-9} m²/s (anions) in 3400 K by Sindzingre *et al.* [9], 3.6×10^{-9} m²/s (anions) in 2900 K by Yamada *et al.* [12]. There has been no experimental study reported about self diffusion coefficient of oxygen near melting points, we could not evaluate our value by comparison with experimental studies. However evaluating our value from other simulation data and simulating liquid state over melting temperature and density, the rigid ion model can be considered reasonable for simulating liquid state.

Figures 3 and 4 show calculated viscosity and thermal conductivity as a function of temperature. The calculated viscosity was smaller than the experimental data by Tsai *et al.* (5–9 mPa·s) and was in good agreement with Woodley's data (4 mPa·s). Although it was considered that calculated viscosity would be large because of the solid behavior of cations, calculated value are within the range of experimental data. Dependency on temperatures was not obtained from our results. The calculated thermal conductivity were several times as large as experimental value by Kim *et al.* and Tasman *et al.*, and moreover they are not smooth with temperature.

The above mentioned disagreement of thermal conductivity and viscosity was because conventional Ewald sum was used for the momentum flow tensor and energy current. The expression for the momentum flow tensor and the energy current include the product term between the interionic distance and force. There remains an ambiguity that a corresponding interionic distance cannot be uniquely defined to an interionic force from the reciprocal space using the conventional Ewald sum. Bernu *et al.* [19] proposed the expression for the Ewald sum in the momentum flow and the energy cur-

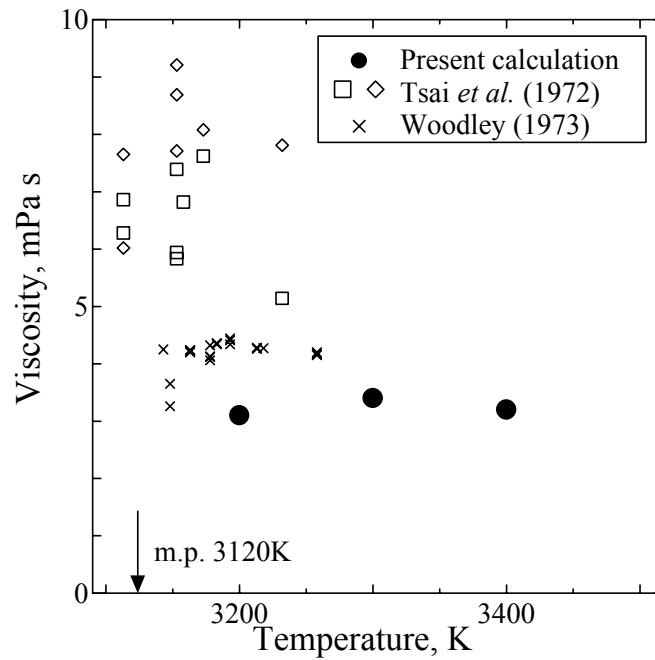


Fig. 3. Calculated viscosity of UO₂ compared with experiments. Filled circles are our results.

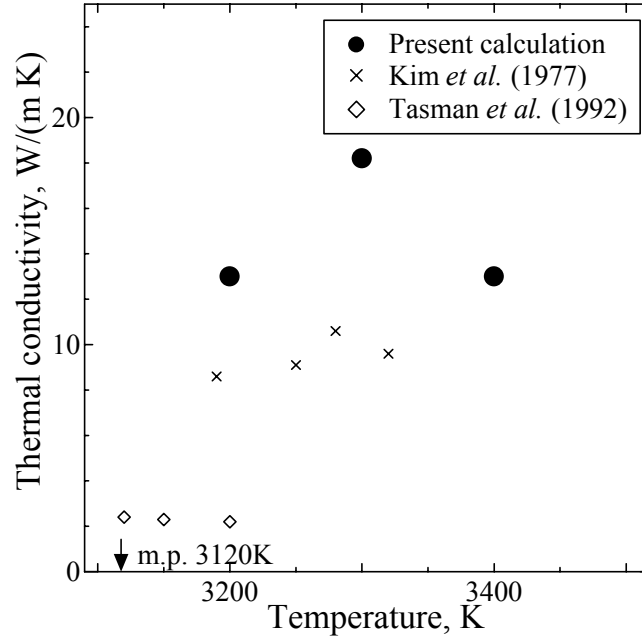


Fig. 4. Calculated thermal conductivity of UO_2 compared with experiments. Filled circles are our results.

rent. Sindzingre *et al.* [20] applied the Ewald sum by Bernu to the calculation of the energy current and calculated thermal conductivities of molten ionic materials such as sodium chloride and potassium chloride by the means of EMD. In order to calculate the viscosity and the thermal conductivity with no ambiguity, we have to apply Ewald sum by Bernu to the longitudinal momentum flow tensor and energy current.

4. CALCULATION RESULTS OF ZIRCONIUM

The potential function of Zr used in the present study is a N -body potential modeled by Willaime *et al* [14]. The contribution of particle i to the cohesive energy Φ_i is

$$\Phi_i = A \sum_{j \neq i}^N \exp \left[-p \left(\frac{r_{ij}}{r_0} - 1 \right) \right] - \sqrt{\xi^2 \sum_{j \neq i}^N \exp \left[-2q \left(\frac{r_{ij}}{r_0} - 1 \right) \right]}, \quad (9)$$

where r_0 is the nearest-neighbor distance in α -Zr at 0 K. Each parameters of the potential are $p=9.3$, $q=2.1$, $A=0.179364$ eV, $\xi=2.2014548$ eV, and $r_0=3.1744$ Å. The repulsive part is a Born-Mayer pairwise interaction and the attractive part is the second-moment approximation of tight-binding band energy.

Since the potential depends explicitly on the interatomic distances only, the interatomic force between particle i and j can be expressed as [21]

$$F_{ij} = \left(\frac{\partial \Phi_i}{\partial r_{ij}} + \frac{\partial \Phi_j}{\partial r_{ij}} \right) \frac{\mathbf{r}_{ij}}{r_{ij}}, \quad (10)$$

$$= \left\{ -\frac{2Ap}{r_0} \exp \left[-p \left(\frac{r_{ij}}{r_0} - 1 \right) \right] + \frac{q\xi}{r_0} \left[\Psi_i^{-1/2} + \Psi_j^{-1/2} \right] \exp \left[-2q \left(\frac{r_{ij}}{r_0} - 1 \right) \right] \right\} \frac{\mathbf{r}_{ij}}{r_{ij}},$$

where

$$\Psi_i = \sum_k^N \exp \left[-2q \left(\frac{r_{ik}}{r_0} - 1 \right) \right]. \quad (11)$$

NVE calculations for Zr were performed for 686 particles. The volume of system was chosen so as to reproduce the experimental density at each temperature [21]. The equations of motions were integrated using the velocity Verlet algorithm with a time step Δt of 2 fs. The kinetic energy was kept at desired temperature with scaling the velocities of all ions for the initial 20 ps. Then the coordinates and velocities obtained for the subsequent 400 ps.

Figure 5 shows the obtained mean square displacement of Zr in 2100 K and 2200 K. The mean square displacement of Zr is convergent to constant value in 2100 K, on the other hand the mean square displacement in 2200 K had large slope. From its results, this model of Zr behaves as liquid state over 2200K. It is confirmed that it can simulate liquid state of Zr adequately because melting temperature of Zr is 2125 K. The calculated self diffusion coefficient was $4.5 \times 10^{-9} \text{ m}^2 \cdot \text{s}^{-1}$. This value was little smaller than the value by Iida *et al.* [22] ($6.8 \times 10^{-9} \text{ m}^2 \cdot \text{s}^{-1}$ at melting point).

Calculated results for viscosity of molten Zr is shown in Fig. 6. We have cal-

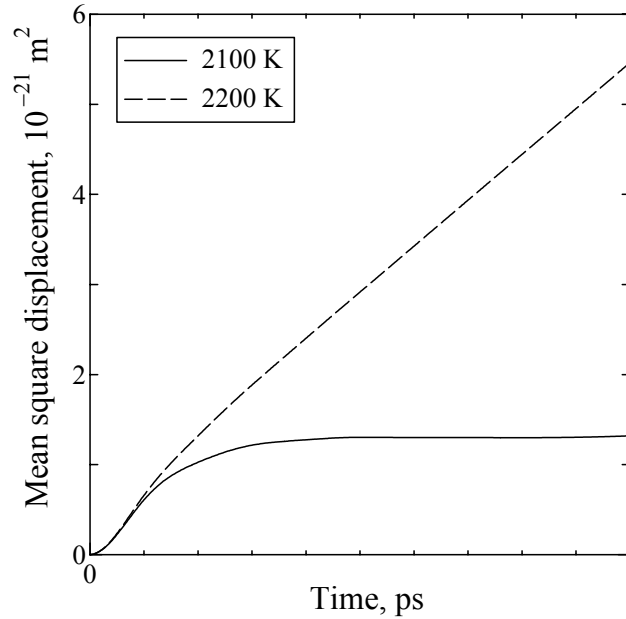


Fig. 5. Calculated mean square displacement of Zr in 2100 K and 2200 K. Solid line; 2100 K, dash line; 2200 K.

culated density of molten Zr for wide range of temperatures up to 2600 K where no experimental data exists. The temperature of molten corium is far over the melting point of Zr. Calculated viscosities with temperature were smaller than other experimental values near melting point: 5 times as small as Bunnell *et al.*, twice as small as Yelviutin *et al.*, 30 % smaller than Paradis *et al.* A little negative dependency of calculated viscosity on temperature was observed from Fig. 7. The negative dependency of viscosity on temperature was smaller than that of Yelviutin data.

Although the potential parameters of Zr were fitted to solid-state properties such as elastic constants, vacancy formation energy, lattice constants, and cohesive energy, the parameters were not fitted to liquid-state properties. To calculate transport properties with higher accuracy, the potential parameters are needed which was fitted to liquid state properties like latent heat and density. Although modeled Zr was fitted only to solid-state properties, we could predict properties in high temperature of metals whose molecular models are complicated if we could model of molecules adequately.

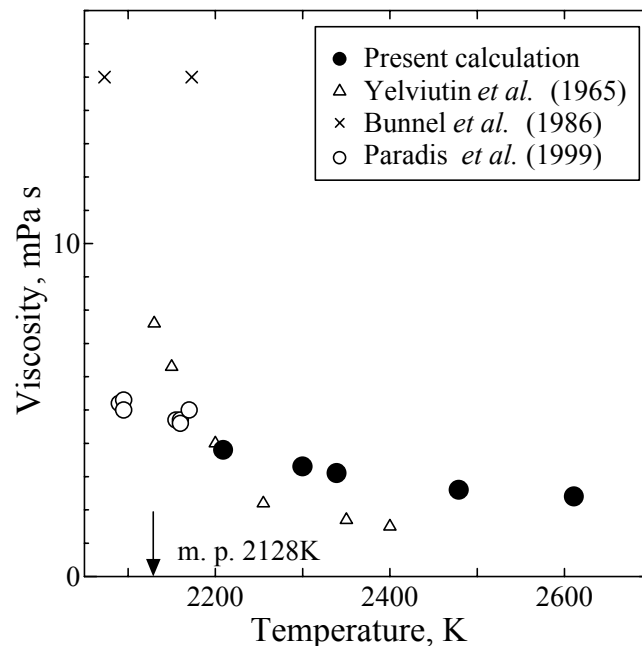


Fig. 6. Calculated viscosity with temperature compared with experimental data. Filled circles are our results.

REFERENCES

1. H. C. Tsai and D. R. Olander, *J. Nucl. Mater.* **44**:83 (1972).
2. R. E. Woodley, *J. Nucl. Mater.* **50**:103 (1974).
3. C. S. Kim, A. Blomquist, J. Fischer, R. Land, M. G. Chasanov, and L. Leibowitz, *Proc. 7th Thermophys. Props.*:338 (1987).
4. H. A. Tasman and D. Daimen, *High Temp. High Press.* **15**:419 (1983).
5. V. P. Yelviutin, M. A. Maurakh, and N. A. Penbkov, *Chernaia Metallurgia* **7**:128 (1965).

6. L. R. Bunnell and J. T. Peter, *Viscosity of zirconium-uranium dioxide (Zr-UO₂) mixtures at 1800 °C to 2100 °C*, (U. S. Nuclear Regulatory Commission Report **NUREG/CRR 4495**, 1986).
7. P. F. Paradis and W. K. Rhim, *J. Mater. Res.* **40**:3713 (1999).
8. A. B. Walker and C. R. A. Catlow, *J. Phys. C: Solid State Phys.* **15**:4061 (1981).
9. P. Sindzingre and M. J. Gillan, *J. Phys. C: Solid State Phys.* **21**:4017 (1988).
10. C. R. A. Catlow, *Proc. R. Soc. A* **353**:533 (1977).
11. P. J. D. Lindan and M. J. Gillan, *J. Phys. Condens. Matter* **3**:3929 (1991).
12. K. Yamada, K. Kurosaki, M. Uno, and S. Yamanaka, *J. Alloys. Comp.* **307**:10 (2000).
13. F. Willaime and C. Massobrio, *Phys. Rev. Lett.* **63**:2244 (1989).
14. G. J. Ackland, S. J. Wooding, and D. J. Bacon, *Phil. Mag. A* **71**:553 (1995).
15. Y. Ida, *Phys. Earth Planet. Interiors* **13**:97 (1976).
16. N. Kumasaka and Y. Nagasaka, *High Temp. -High Press.* **33**:911 (2001).
17. J. K. Fink, *J. Nucl. Mater.* **279**:1 (2000).
18. T. Karakasidis and P. J. D. Lindan, *J. Phys. Condens. Matter* **6**:2965 (1994).
19. B. Bernu and P. Vieillefosse, *Phys. Rev. A* **18**:2345 (1978).
20. P. Sindzingre and M. J. Gillan, *J. Phys. Condens. Matter* **2**:7033 (1990).
21. V. Rosato, M. Guillope, and B. Legrand, *Phil. Mag. A* **59**:321 (1989).
22. T. Iida and R. G. Roderick, *The Physical Properties of Liquid Metals*, (Oxford, Clarendon Press, 1988).